Visibility and Raman spectroscopy of mono and bilayer graphene on crystalline silicon

Emil B. Song,[1,a)] Bob Lian,[1] Guangyu Xu,[1] Bo Yuan,[2] Caifu Zeng,[1] Amber Chen,[1] Minsheng Wang,[1] Sungmin Kim,[1] Murong Lang,[1] Yi Zhou,[1] and Kang L. Wang[1]
[1]*Department of Electrical Engineering, University of California, Los Angeles, California 90095, USA*
[2]*Department of Computer Science, University of California, Los Angeles, California 90095, USA*

(Received 24 December 2009; accepted 27 January 2010; published online 23 February 2010)

Experimental studies of pristine graphene devices currently rely on the fact that the graphene crystallites can be visible under optical microscopes when the underlying substrate is engineered to exhibit high contrast. Here, we present that graphene can be visualized not only on a dielectric substrate but also on a crystalline Si surface of a silicon-on-insulator (SOI) wafer (SIMOX and Bonded) with thicknesses of Si ~70 nm and buried oxide ~140 nm, using monochromatic illumination. In addition, we have found that Raman spectroscopy shows similar features to standard graphene on SiO_2 substrates independent of the polarity of the Si surface. Finally, the Raman spectrum on SOI exhibits a higher intensity compared to that on bulk Si due to the interference enhancement effect of graphene on SOI. Thus, the usage of optical microscopy and Raman spectroscopy for detecting, locating, and characterizing graphene serves as a high throughput method to further study graphene on semiconductor systems and other substrates beyond SiO_2/Si. © *2010 American Institute of Physics*. [doi:10.1063/1.3323105]

Graphene, due to its outstanding electrical[1,2] properties, has been considered as a promising candidate for future electronic devices in integrated circuits. For the past few years, extensive studies have been conducted by exfoliating graphene only onto specific dielectrics since the underlying substrates limits graphene's visibility[3,4] and characterization methods.[5] Certain attempts were made to put graphene on semiconductor substrates in order to examine substrate-induced effects,[6,7] the morphology, and flexibility of graphene.[8] However, the lack of a high throughput method to detect and characterize graphene on a semiconductor substrate hinders further studies pertinent to graphene/semiconductor junctions, which are compatible with current semiconductor devices. Furthermore, easy access to graphene/semiconductor heterostructures could provide a platform for unprecedented device structures[9] and accelerate graphene application for future technology.

Here, we present a method to detect graphene visibly on a silicon-on-insulator (SOI) substrate, and show Raman spectroscopy as an effective characterization tool in identifying MLG and BLG. The graphene samples were prepared by micromechanical cleavage on a SIMOX (Separation by IMplanted OXygen) SOI, Bonded SOI, and 320 nm SiO_2 wafer. The thicknesses of the Si/SiO_2 layers for SIMOX and Bonded SOI are 70 nm/140 nm and 70 nm/145 nm, respectively. An optical microscope with a variable interference filter of FWHM=10 nm was used to locate the MLG and BLG, and micro Raman spectroscopy was used to characterize the graphene samples.

Figure 1 illustrates the optical image depending on different wavelengths of light. Graphene is nearly invisible in the blue and green region of the visible spectrum and only becomes detectable under red wavelengths near 600 nm. The 600 nm light has a penetration depth ($\delta_{pen}=1/\alpha_{abs}$) of 1.8 μm in silicon, that allows 96% of the incident light to transmit through the top 70 nm Si layer, and create a resonant condition in the buried oxide (BOX) layer for high contrast. Small circular dimples on the SOI substrates are noticed

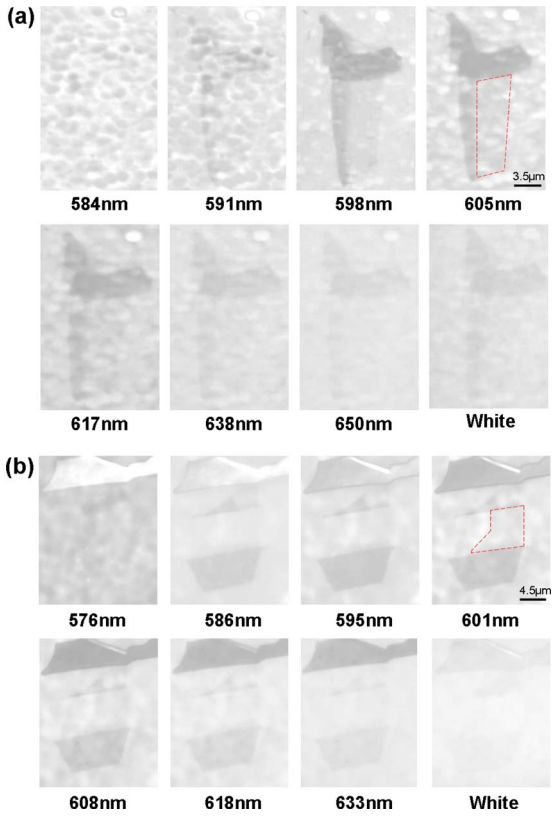

FIG. 1. (Color online) Optical images of graphene on SOI. (a) MLG on SIMOX SOI with different wavelengths of illumination. Scale bar: 3.5 μm (b) MLG on Bonded SOI. Scale bar: 4.5 μm. The enclosed area of the dotted line is MLG. The images are illuminated through a narrow bandpass filter (variable interference filter).

[a)]Electronic mail: emil@ee.ucla.edu.

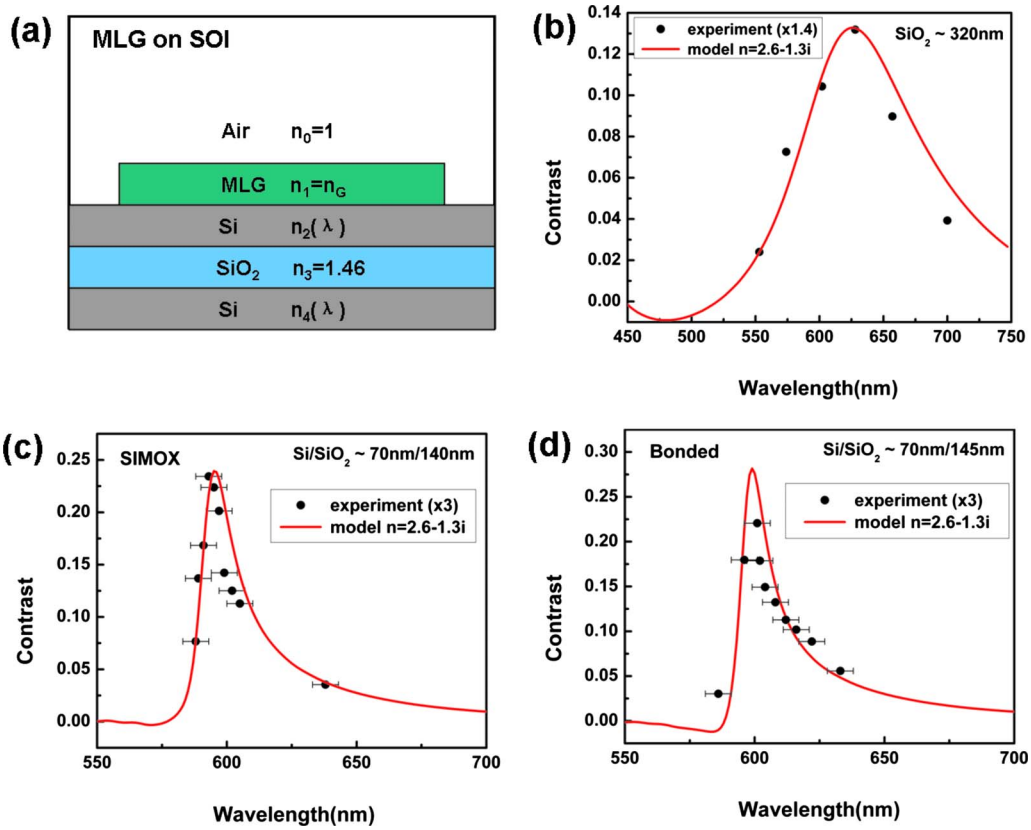

FIG. 2. (Color online) Contrast of graphene on SOI depending on wavelength. (a) Four-layer structure of MLG on SOI. (b) Contrast of MLG on SiO_2. (c) Contrast of MLG on SIMOX SOI. (d) Contrast of MLG on Bonded SOI. The error bars represent the FWHM=10 nm of the variable interference filter. The experimental values show good agreement with the simulation upon multiplying a constant as shown in each figure.

able; these imperfections arise from the stochastic process of implantation and the annealing procedure during processing of the SOI wafer.[10]

Figure 2 displays a quantitative analysis accompanied with the simulation result. The theoretical contrast was estimated using the Fresnel's model of a four layer system [Fig. 2(a)] upon normal incidence. The contrast is defined as $1-I_G/I_{Si}$, where I_G and I_{Si} are the reflected intensity with and without graphene of the SOI substrate, respectively. The reflected light intensity is as follows:[11]

$$I(\lambda)=\left|\frac{r_1+r_2e^{-i\Delta_1}+r_3e^{-i(\Delta_1+\Delta_2)}+r_4e^{-i(\Delta_1+\Delta_2+\Delta_3)}+r_1r_2r_3e^{-i\Delta_2}+r_1r_3r_4e^{-i\Delta_3}+r_1r_2r_4e^{-i(\Delta_2+\Delta_3)}+r_2r_3r_4e^{-i(\Delta_1+\Delta_3)}}{1+r_1r_2e^{-i\Delta_1}+r_1r_3e^{-i(\Delta_1+\Delta_2)}+r_1r_4e^{-i(\Delta_1+\Delta_2+\Delta_3)}+r_2r_3e^{-i\Delta_2}+r_3r_4e^{-i\Delta_3}+r_2r_4e^{-i(\Delta_2+\Delta_3)}+r_1r_2r_3r_4e^{-i(\Delta_1+\Delta_3)}}\right|^2,$$

where $r_i=(n_{i-1}-n_i)/(n_{i-1}+n_i)$ are the reflection coefficients for interfaces between layer i and $i-1$, and $\Delta_j=4\pi n_j d_j/\lambda$ is the path difference for layer j. $d_G=0.34$ nm (extension of the π-orbital) and $n_G=2.6-1.3i$ was used for the thickness of MLG and the complex refractive index, respectively.[3]

The contrast value was extracted using a two-dimensional averaging technique instead of a one-dimensional line analysis due to the circular dimples and domains. The discrepancies of the extracted contrast values stem from the use of bulk graphite's optical constant for graphene and ignoring the angle dependent reflection of the conical-shaped light exiting the objective lens. The inferior image quality from the dimples and domains on SOI also decreases the contrast.

Raman spectroscopy of MLG on SIMOX substrates, depending on the polarity of the silicon surface (100), was investigated [Fig. 3(a)]. Measurements were performed at 514 nm with <2 mW (0.5 mW/μm^2) incident power to minimize any spectral change from heat.[5] The nonpolar hydrogen terminated surface was prepared by removing the native oxide layer with hydrofluoric acid, immediately followed by exfoliation of natural graphite. The peak position and FWHM of the doubly degenerate G band (Pos ~1580 cm^{-1}, FWHM~10 cm^{-1}) and the double resonant 2D band (Pos~2680 cm^{-1}, FWHM~26 cm^{-1}) of MLG do not exhibit any noticeable difference between hydrogen (nonpolar) and oxygen terminated (polar) silicon surfaces. Moreover, no considerable change in the peak positions and FWHM was detected in comparison with SiO_2 substrates. This implies that the Raman excitations are decoupled with the silicon surface when adhered through mechanical exfoliation,[7] which is not the case for epitaxial graphene that shows stress induced effects originating from the SiC substrate.

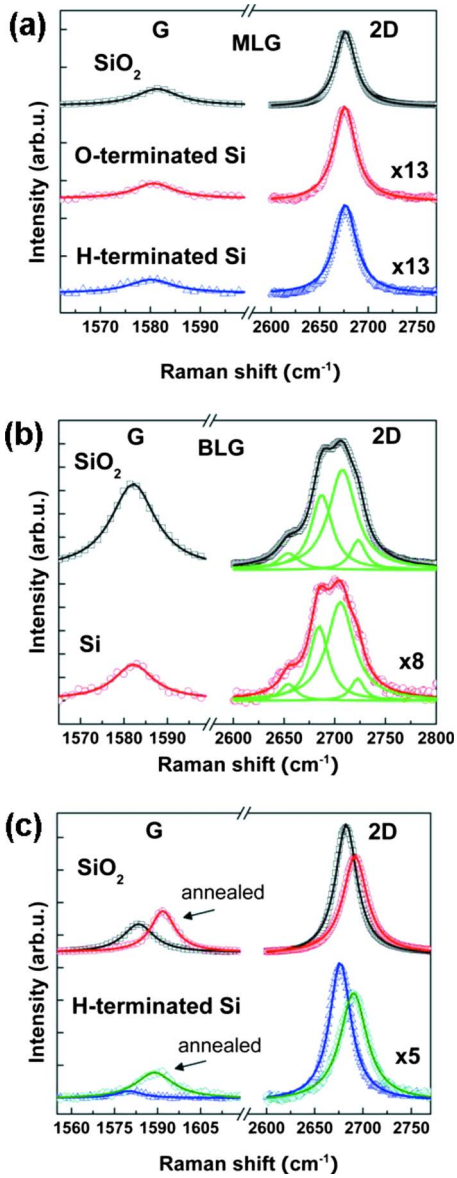

FIG. 3. (Color online) Raman spectroscopy (RS) of graphene on SOI. (a) RS of MLG depending on the polarity of Si surface. (b) RS of BLG on Si. The 2D band is fitted with four Lorentzian functions. (c) RS of MLG before and after H_2/Ar annealing at 300 °C. RS of graphene on SiO_2 are illustrated as reference. The Raman was taken at a condition of 600s acquisition time with less than 2 mW laser power. The Raman intensity for Si substrates are enhanced by a factor as indicated on each spectrum.

In the case of the BLG on SOI [Fig. 3(b)], the 2D band was accurately fitted with four Lorentzian functions ($Pos^1 \sim 2654\ cm^{-1}$, $Pos^2 \sim 2685\ cm^{-1}$, $Pos^3 \sim 2706\ cm^{-1}$, and $Pos^4 \sim 2723\ cm^{-1}$) akin to BLG on a SiO_2 substrate;[5] the four peaks depict the band structure of a BLG through the double resonant process. This allows the 2D band of graphene to be an excellent characterization tool for determining the number of layers on a silicon substrate. Although the Raman intensity of graphene on SOI diminishes by an order of magnitude in comparison to graphene on SiO_2, it has increased by approximately one order of magnitude compared to that on bulk Si substrate.[12] The constructive interference of the excitation laser and Raman signal within the multilayer structure is not optimized, but sufficient for the Raman intensity to enhance.[12]

The carrier concentration of graphene can also be monitored through Raman spectroscopy from the removal of the Kohn anomaly.[13,14] In order to detect charge transfer effects arising from the work function difference between graphene $\Phi_{graphene} \sim 4.5$ eV[15] and the boron doped $(5 \times 10^{15}/cm^3)$ silicon $\Phi_{Si} \sim 4.97$ eV, the graphene sample on the H-terminated silicon surface was annealed in H_2 (50%)/Ar (50%) at 300 °C for 20 min to improve the graphene/silicon interface.[16] The graphene on SiO_2 was also annealed with the same condition for comparison. Fig. 3(c) shows, however, that the Raman spectrum of both MLG on Si and SiO_2 blue shifts ($G_{Si} \rightarrow 1590\ cm^{-1}$ and $2D_{Si} \rightarrow 2690\ cm^{-1}$; $G_{SiO2} \rightarrow 1592\ cm^{-1}$ and $2D_{SiO2} \rightarrow 2692\ cm^{-1}$), which corresponds to a hole doping of approximately $10^{13}/cm^2$ independent of the substrate.[13] Two possible reasons for phonon stiffening of MLG on Si are hole transfer from the p-doped silicon substrate and hole doping from the atmospheric adsorbates after thermal treatment. The dominant source for MLG on SiO_2, however, is the latter.[17] This makes the origin of stiffening for MLG on Si difficult to differentiate between the two effects.

In summary, high throughput methods such as optical microscopy and Raman spectroscopy can be used for detecting and identifying mono and BLG on crystalline silicon. This will expedite the process to make structures for understanding junction properties of graphene/semiconductors and provide opportunities to engineer hybrid device structures.

The authors would like to thank S. Bedell from IBM and B.Y. Nguyen from SOITEC for providing the SIMOX SOI and Bonded SOI substrates, respectively. This work has been partially supported by Functional Engineered Nano Architectonics (FENA) which is funded through the Focus Center Research Program, and the NSF-IGERT (DGE-0114443) program (E.B.S.).

[1] K. S. Novoselov, A. K. Geim, S. V. Morozov, D. Jiang, Y. Zhang, S. V. Dubonos, I. V. Grigorieva, and A. A. Firsov, Science **306**, 666 (2004).
[2] K. I. Bolotin, K. J. Sikes, Z. Jiang, M. Klima, G. Fudenberg, J. Hone, P. Kim, and H. L. Stormer, Solid State Commun. **146**, 351 (2008).
[3] P. Blake, E. W. Hill, A. H. C. Neto, K. S. Novoselov, D. Jiang, R. Yang, T. J. Booth, and A. K. Geim, Appl. Phys. Lett. **91**, 063124 (2007).
[4] G. Teo, H. Wang, Y. Wu, Z. Guo, J. Zhang, Z. Ni, and Z. Shen, J. Appl. Phys. **103**, 124302 (2008).
[5] A. C. Ferrari, J. C. Meyer, V. Scardaci, C. Casiraghi, M. Lazzeri, F. Mauri, S. Piscanec, D. Jiang, K. S. Novoselov, S. Roth, and A. K. Geim, Phys. Rev. Lett. **97**, 187401 (2006).
[6] I. Calizo, W. Bao, F. Miao, C. N. Lau, and A. A. Balandin, Appl. Phys. Lett. **91**, 201904 (2007).
[7] Y. y. Wang, Z. h. Ni, T. Yu, Z. X. Shen, H. m. Wang, Y. h. Wu, W. Chen, and A. T. Shen Wee, J. Phys. Chem. C **112**, 10637 (2008).
[8] U. Stöberl, U. Wurstbauer, W. Wegscheider, D. Weiss, and J. Eroms, Appl. Phys. Lett. **93**, 051906 (2008).
[9] Z. Jing and J. C. S. Woo, International Conference on Solid-State Device and Materials, Sendai, Japan 2009, pp. 1226–1227.
[10] S. Hahn, K. Kugimiya, K. Vojtechovsky, M. Sifalda, M. Yamashita, P. R. Blaustein, and K. Takahashi, Semicond. Sci. Technol. **7**, A80 (1992).
[11] H. Anders, *Thin Films in Optics* (Focal, London, 1967), pp. 47–59.
[12] L. Gao, W. Ren, B. Liu, R. Saito, Z.-S. Wu, S. Li, C. Jiang, F. Li, and H.-M. Cheng, ACS Nano **3**, 933 (2009).
[13] A. Das, S. Pisana, B. Chakraborty, S. Piscanec, S. K. Saha, U. V. Waghmare, K. S. Novoselov, H. R. Krishnamurthy, A. K. Geim, A. C. Ferrari, and A. K. Sood, Nat. Nanotechnol. **3**, 210 (2008).
[14] S. Piscanec, M. Lazzeri, F. Mauri, A. C. Ferrari, and J. Robertson, Phys. Rev. Lett. **93**, 185503 (2004).
[15] G. Giovannetti, P. A. Khomyakov, G. Brocks, V. M. Karpan, J. van den Brink, and P. J. Kelly, Phys. Rev. Lett. **101**, 026803 (2008).
[16] R. R. Razouk and B. E. Deal, J. Electrochem. Soc. **129**, 806 (1982).
[17] L. Liu, S. Ryu, M. R. Tomasik, E. Stolyarova, N. Jung, M. S. Hybertsen, M. L. Steigerwald, L. E. Brus, and G. W. Flynn, Nano Lett. **8**, 1965 (2008).